Molecular Dynamics Simulations of Perylene and Tetracene Librations: Comparison With Femtosecond Upconversion Data

Tilman Rosales,[†] Jianhua Xu,[†] Xiongwu Wu,[‡] Milan Hodoscek,[‡] Patrik Callis,[§] Bernard R. Brooks,[‡] and Jay R. Knutson*,[†]

Optical Spectroscopy Section, Laboratory of Molecular Biophysics, National Heart, Lung and Blood Institute, National Institutes of Health, Building 10-Magnuson CC, 5D14, 10 Center Dr, Bethesda, Maryland 20892, Laboratory of Computational Biology, National Heart, Lung and Blood Institute, National Institutes of Health, Bethesda, Maryland 20892, and Department of Chemistry & Biochemistry, Montana State University, Bozeman, Montana 59717

Received: December 13, 2007; Revised Manuscript Received: March 14, 2008

In a prior manuscript by Xu et al. [Xu, J.; Shen, X.; Knutson, J. R. *J. Phys. Chem. A* **2003**, *107*, 8383], time-resolved fluorescence emission anisotropy measurements were performed on perylene and tetracene in hexadecane using an upconversion technique with ~100 fs resolution. The anisotropy transients contained previously unseen decay terms of ~300 fs. In perylene, their amplitude corresponded to the "r_o defect" that has gathered interest over decades. We ascribed this term to a predominantly in-plane libration. In this manuscript, we present molecular dynamics simulations for the motions of perylene and tetracene using the CHARMm molecular dynamics program (version c29b2). Both rotational correlation functions contain subpicosecond decay terms that resemble experimental anisotropy decays. It was suggested that the r_o defect might arise from excited-state distortions of perylene, so we conducted quantum mechanical calculations to show that such distortion does not significantly displace the oscillators. We compare the case of perylene, with a strongly allowed singlet emission transition, to that of the weakly allowed tetracene transition. In perylene, motion alone can explain subpicosecond anisotropy decay, while tetracene decay also contains vibrational coupling terms, as previously reported by Sarkar et al. [Sarkar, N.; Takeuchi, S.; Tahara, T. *J. Phys. Chem. A* **1999**, *103*, 4808].

1. Introduction

Hydrodynamic theory for molecules in solution is often separated into two categories, depending on the boundary conditions imposed on the interaction between the solvent and the solute. "Stick" boundary conditions are applied when the solute "drags" some of the solvent molecules with it as it diffuses in the solvent, usually imposed when the solute is larger than the solvent, so the solvent exhibits continuum behavior. Since hydrogen bonding is prolific, solvation in water is usually considered to cause "stick" boundary conditions. "Slip" boundary conditions apply when the solvent "rolls" on the surface of the solute and there is very little interaction between the two, usually occurring when the solute and solvent are about the same size. An example is solvation in hydrocarbons of smaller hydrophobic solutes. Since there is very little interaction between solute and solvent, small rotations can occur that are accompanied by very little physical displacement of the solvent.

Fluorescence spectroscopy can be used to measure the rotational diffusion of molecules by following the emission anisotropy decay of the species in solution. A brief light pulse is used to excite the molecules, photoselecting a population whose oscillators are mostly aligned with the excitation polarization axis. The emission anisotropy decay is due to the ensemble of fluorescing molecules losing this initial alignment (esp. due to rotational diffusion), and it is often seen to decay multiexponentially. In nonviscous solvents, these motions occur in tens of picoseconds, so one needs very fast probing techniques in order to observe small molecules rotating in solution.

If we model molecules as ellipsoids of revolution, rotation about the unique axis in either a "prolate" or an "oblate" object is called $D_{\|}$ and the rotation along either of the other axes is referred to as $D_{\perp}$. As shown in eq 1, the emission anisotropy decay of a general rigid ellipsoid is described by a sum of five exponential terms:[3]

$$r(t) = \sum_{i=1}^{5} \beta_i \exp(-t/\phi_i) \tag{1}$$

where β_i are trigonometric functions of the angles between the transition dipoles and the symmetry axis of the ellipsoid, and ϕ_i are the rotational correlation times. Additionally, we can make the simplification that these five correlation times collapse to three for an axisymmetric ellipsoid; they are given by eq 2:[3]

$$\begin{aligned} \phi_1^{-1} &= 6D_{\perp} \\ \phi_2^{-1} &= 2D_{\perp} + 4D_{\|} \\ \phi_3^{-1} &= 5D_{\perp} + 1D_{\|} \end{aligned} \tag{2}$$

Note that the first and third correlation times are very close to each other, making them practically indistinguishable. Hence, the anisotropy for an axisymmetric ellipsoid can be described adequately with two amplitudes and two rotational correlation times.[4]

* Corresponding author. E-mail: jaysan@helix.nih.gov. Phone: (301) 496-2557. Fax: (301) 480-4625.

[†] Laboratory of Molecular Biophysics, National Heart, Lung and Blood Institute, National Institutes of Health.

[‡] Laboratory of Computational Biology, National Heart, Lung and Blood Institute, National Institutes of Health.

[§] Montana State University.

10.1021/jp7117289 CCC: $40.75
Published on Web 05/29/2008

Time-resolved fluorescence anisotropy measurements are widely used to provide information on the dynamics of molecules in solution, and it has recently been extended down to femtosecond resolution. The anisotropy decay of a system, $r(t)$, is still calculated in the same way:[5,6] $r(t)$ is obtained from measurements of the decays with parallel and perpendicular polarization with respect to the excitation direction.

$$r(t) = \left(\frac{I_{||}(t) - I_{\perp}(t)}{I_{||}(t) + 2I_{\perp}(t)}\right) \tag{3}$$

The theoretical limit for the initial anisotropy, r_o, is 0.4 for single photon electronic transitions in fluorophores. An anisotropy of 0.4 indicates that the absorption and emission moments are collinear:

$$r_o = 0.2(3\cos^2\beta - 1) \tag{4}$$

where β is the angle between the absorption and emission transition moments. If instead of this intramolecular angle between oscillators, we use γ as the angle between the initial excitation axis and the ultimate emission axis at time t, we obtain the emission anisotropy decay function for the ensemble:

$$r(t) = \langle 0.2(3\cos^2\gamma(t) - 1)\rangle \tag{5}$$

Perylene (an oblate molecule) and tetracene (a prolate molecule) are planar molecules that have well defined "in-plane" and "out-of-plane" rotations.[7] Prior experiments with ~100 ps resolution have frequently yielded $r_o < 0.4$, the so-called "r_o defect".[4] The rotational relaxations of perylene and tetracene in hexadecane and glycerol have been measured in our laboratory using femtosecond upconversion fluorescence spectroscopy.[1] The theoretical value of 0.4 cannot be attained when this data is fit with a biexponential model. A third apparent rotation fit with an exponential of ~500 fs has been found that is essentially independent of temperature and viscosity. This very fast rotation was believed to mostly be due to an "in-plane" femtosecond libration of the molecules within their solvent pockets. The source of libration has not been determined, so we have used molecular dynamics (MD) simulations to determine if it is a reasonable consequence of rotations that yield little solvent displacement.

MD is a classical computational method that calculates the time-dependent behavior of a system. It is used to determine detailed information of the movement of molecules in solution including conformational changes. MD simulations provide a microscopic picture of molecular diffusion.[8] A direct application of this method is to obtain rotational relaxation data from the angular correlation function. The angular correlation function is defined as

$$C_2(t) = \frac{\langle 3(\vec{n}(0)\cdot\vec{n}(t))^2 - 1\rangle}{2} \tag{6}$$

where $\vec{n} = (n_x, n_y, n_z)$ is a vector rotating with the molecule at time t. For excitation and emission oscillators aligned along the same molecular axis, anisotropy decay can be related to the correlation function by

$$r(t) = \frac{2}{5}C_2(t) \tag{7}$$

Here $C_2(t)$ is the angular correlation function of the emission dipole. Since we are approaching the same time scale as solvent−solute collisions, the libration that we seek to describe might not follow an exponential decay; instead, it might have quasi-ballistic behavior.[9]

Perylene is an ideal molecule for these studies, since it is amenable to excitation into states with different initial transition moment directions (i.e., $\beta = 0$ or $\sim\pi/2$ in eq 4 above). The model of perylene as a rigid molecule was used initially in our MD calculations, because fluorescence depolarization theory only applies to a rigid ellipsoidal molecule. Perylene has previously been observed to follow stick boundary conditions in one type of solvent and then follow slip-like behavior in other solvents.[10] Further, perylene has been shown to transition from apparent stick boundary conditions to slip boundary conditions as the length of solvent in an n-alkane series is increased.[11] It is also known that perylene becomes more rigid in the first excited state,[12] helping to justify our use of a rigid perylene molecule in the MD simulations.

With femtosecond upconversion experiments, we are able to obtain a clearer picture of molecules in solution and are now able to time-resolve most of the "r_o defect" previously seen and speculated about by many researchers. We can probe the first few picoseconds in great resolution when compared to previous analyses of perylene anisotropy.[4−6,8,13,14] Upconversion analysis permits very fast motion of molecules in solution to be observed, down to perhaps 15% of laser pulse widths, which may themselves be ~200 fs. Probe molecules such as perylene may contain in their motions details of solvent structure around the solute that could not be observed with picosecond or nanosecond resolution.[8,10,15] Perylene and tetracene have previously demonstrated subslip (faster than slip) behavior in alcohols that was explained in the context of local solvent structures.[16,17] At these short time scales, there is free rotation with little solvent displacement ("libration"). The sort of solvent pockets shown by Jas[8] et al. are snapshots of the average environment around the solute. There is clearly an opportunity for libration of a few degrees taking r from 0.4 to ~0.36; subsequent rotations, however, require restructuring and reforming of the pocket around the solute. The conceptual separation of these motions is somewhat artificial, as the time scales of solute libration and solvent diffusion overlap.

Other explanations for the possible r_o defect that we consider are vibrational coupling, reported by Sarkar[2] et al. for tetracene and the work by Szubiakowski[18] et al. that examined the possible nonplanarity[19] of perylene in either the ground or first excited states. We present simulations of perylene and tetracene in a hexadecane box using MD, and we compare the results to our earlier upconversion anisotropy data.[1]

2. Methods

2.1. Simulations. We used the CHARMM[20] (Chemistry at HARvard Molecular Mechanics, version c29b2) program in order to obtain information that will help us determine the source of the "libration", including autocorrelation functions and thermodynamic properties. This study utilized the high-performance computational capabilities of the Biowulf PC/Linux cluster at the National Institutes of Health, Bethesda, MD (http://biowulf.nih.gov). The charges and topology of perylene are taken from Jas et al.[18] The geometry optimized structure of tetracene was used. Using Gaussian 03,[21] the tetracene structure was minimized, and the atomic charges were obtained from the Mulliken population analysis of the HF/6−31G* optimized structure. Using CHARMM, geometry optimizations were performed on the pure solvent alone. We used a dodecahedral box with periodic boundary conditions. In all molecular simulations, SHAKE constraints were introduced on the bonds involving hydrogen atoms. Integration of Newton's equations of motion was carried out with the Verlet leapfrog algorithm

with a time step of 0.002 ps. In all energy calculations, a 14.0 Å atom based nonbonded cutoff distance was used, with a switching function between 8.0 and 12.0 Å for van der Waals terms and a force shift function at 12.0 Å for electrostatics. The nonbonded neighbor atom lists were generated every 40 steps. The temperature was held at 300 K for all the simulations, with a window of 5 K. The solute was placed in the center of the dodecahedral box, and those solvent molecules that overlapped the solute were removed. The solution boxes contained one solute molecule in 508 hexadecane molecules in a cell based on a cube of side 71.05 Å. We then performed simulations corresponding to the NVT ensemble with the solute fixed to allow the solvent to rearrange around the solute. The simulations were carried out for 1 ns. The temperature was held constant using velocity rescaling. Production dynamics simulations on the whole system were performed in order to extract correlation functions and hydrodynamic properties to compare with femtosecond experimental data. The simulation was performed in the NPT ensemble. The average pressure was held at 1 atm using the Langevin piston method, with a piston mass of 500.0 amu and a collision frequency of 20 ps^{-1}. The average temperature was held constant using the Hoover algorithm with a coupling parameter of 1000 kcal ps^2 and a reference temperature of 300 K. Trajectories were saved every 0.1 ps for 1 ns simulation time. We used the movement of the symmetry axes of the molecules over time to determine the correlation times. A vector along the central carbons in the plane of the molecule or a vector normal to the plane was used to obtain the angular correlation function in the simulations for the "in-plane" or "out-of-plane" results, respectively.

2.2. Quantum Mechanics. The quantum mechanical calculations were done with Gaussian 03. The NIH SGI Origin 3400 supercomputer, known as Nimbus, was used, which runs the IRIX 6.5 operating system. The crystal structure was optimized using B3LYP/6-31G** calculated energies. Normal modal frequencies of perylene were found after optimization. Two conformations with the lowest energy were chosen. They represent the butterfly and twisted conformations that have been described elsewhere.[12,22] These two conformations were visualized, and their energies were increased by 4kT using MOLDEN (v3.6).[23] The exact energies were calculated by the Hartree−Fock (HF) method using a 6-31G* basis set. The coordinates of maximum displacement of each conformation after the addition of energy were used for the calculation of the excited energies and the transition moments. The excited states are obtained by single excitations from the closed shell ground state. The calculation on excited states was done using the CIS (CI-Singles) and Dunning's correlation consistent double basis set (cc-pVDZ) in Gaussian 03. A full population analysis was performed with Gaussian. In this way, transition moments were obtained for both conformations.

3. Results

The radii of gyration of both perylene and tetracene are found to be of the same order as hexadecane, implying perylene and tetracene should fall into the "slip" regime. Perylene will initially displace little solvent as it rotates "in-plane", leading to the expectation that this rotation is quasi-ballistic in nature with very little friction. Figure 1 shows the experimental data and simulation of perylene in hexadecane. A third exponential term was used to empirically fit our prior data to account for the defect in initial anisotropy, r_o. The data was fit with $r(t) = 0.24\ \exp(-t/21) + 0.1\ \exp(-t/130) + 0.05\ \exp(-t/0.45)$, where times are in picoseconds. Notice that the MD simulation

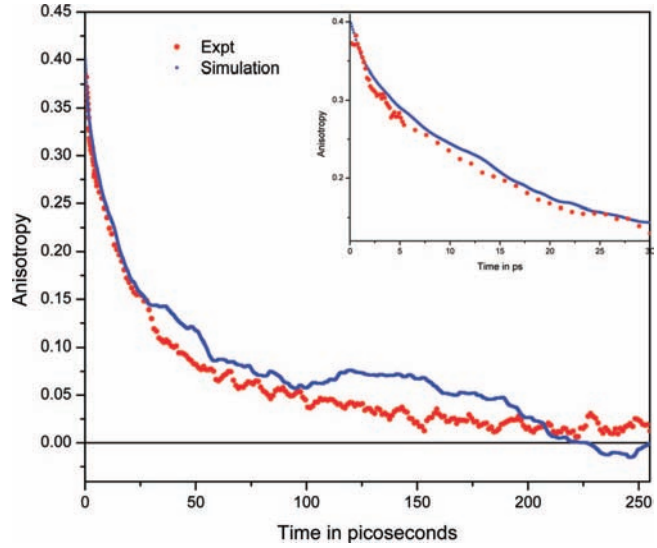

Figure 1. Femtosecond anisotropy decay of perylene in hexadecane (●,red). The published experimental data was fitted adequately with $r(t) = 0.24\ \exp(-t/21) + 0.1\ \exp(-t/130) + 0.05\ \exp(-t/0.45)$, where times are in picoseconds. The first 250 ps of the simulation are also shown (■, blue). The total simulation time was 4 ns. The inset has the first 30 ps.

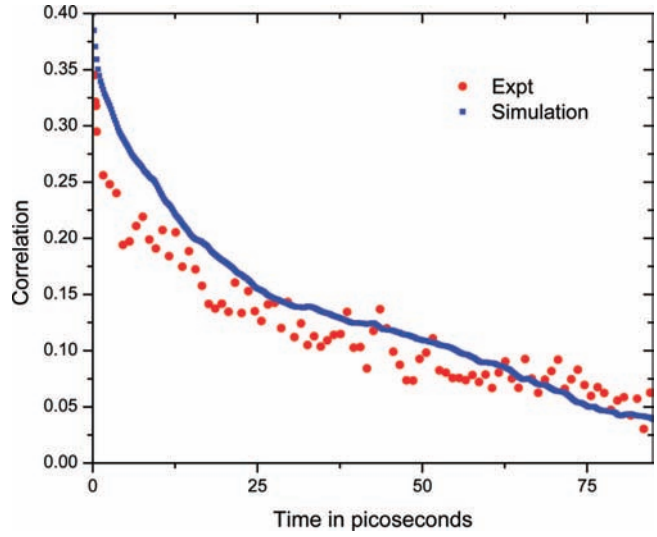

Figure 2. Tetracene in hexadecane anisotropy decay (●, red). The data was fitted adequately with $r_0(t) = 0.27\ \exp(-t/10) + 0.08\ \exp(-t/160) + 0.03\ \exp(-t/0.6)$, where times are in picoseconds. Also shown is the tetracene in hexadecane anisotropy simulation (■, blue). Note the experimental $r(0)$ value does not reach the value of 0.4, but qualitatively the decay is similar. See text for details.

is able to faithfully predict the initial anisotropy decline seen in perylene experiments. The inset focuses on the first 30 ps of the perylene in hexadecane simulation, where we can clearly see the initial behavior corresponding to the "libration" in both the experiment and simulation. Figure 2 shows the first 75 ps of the experimental anisotropy decay data of tetracene excited at 410 nm (the 0−2 band) in hexadecane and the corresponding tetracene in hexadecane simulation. The simulations reproduce features of tetracene anisotropy decay only qualitatively. Some of the mismatch may originate in the limited time resolution of the laser pulse generating that experimental data. Convolution with the broader "instrument response function" at this wavelength may prevent r from reaching 0.4, and the simulation also appears horizontally offset. Nevertheless, we clearly see a

Figure 3. The two conformations of perylene studied: butterfly and twisted. 4 kT of energy was added to each conformation. The conformation shown is that of maximum displacement from a flat perylene with 4 kT of energy.

TABLE 1: The Transition Moments (in AU) and Oscillator Strengths Obtained From the Quantum Mechanical Calculations for the First Three Excited States of Both Heavily Distorted Perylene Configurations (Twisted and Butterfly)

	TMx	TMy	TMz	oscillator strength (f)	angle from symmetry axis
			Twisted		
1	2.800	0.000	0.0000	0.7021	~6.0°
2	0.000	0.000	0.0497	0.0003	
3	0.000	0.000	0.0376	0.0002	
			Butterfly		
1	2.7668	0.003	0.0000	0.6916	~5.0°
2	0.0000	0.0000	0.0000	0.0000	
3	0.0000	0.0000	0.0000	0.0000	

subpicosecond, predominantly in plane rotation, ("libration") in the simulations.

Unlike perylene with strong allowed transitions,[24] which we show to lie only on the symmetry axes, tetracene (with weakly allowed S_1-S_o[25]) has been shown by Sarkar[2] to have anisotropy decay contaminated with picosecond changes in vibrational coupling between S_1 and S_n states. We initially discounted the effect of such coupling when inspecting experimental anisotropy decay data[1] like that seen in Figure 2, but recently we confirmed the results of Sarkar in the ultraviolet and also found that excitation at 442nm (in the 0−1 band) yielded $r(t)$ curves with $r_o < 0.4$ that differ from Figure 2 (data not shown). Hence the comparison in Figure 2 cannot be expected to be quantitative as in Figure 1; in fact, a model combining libration and vibrational cooling would be required to fully rationalize tetracene. As that is beyond the scope of this manuscript, we include Figure 2 only to show the potential contribution of a libration to that anisotropy decay profile.

Figure 3 shows the twisted and butterfly conformations of perylene used for the calculations of the transition moments (shown with their maximum displacement from a flat perylene). They are shown displaced about 6° and 5° from the symmetry axis, respectively. In Table 1, we can see that even at 4 kT of energy away from equilibrium, the direction of the transition moment is essentially along the long axis in the plane of the molecule (TMx), while the transition moment perpendicular to the plane (TMz) is negligible for the first three excited states of both twisted and butterfly conformations. Further, the oscillator strengths for those excited states with nonzero TMz are negligible. Since our calculation of transition moments inside the distorted molecule do not deviate significantly from the x-axis, we expect that even the excited-state of perylene (with excess vibrational energy) will remain x-axis polarized. Our calculations find little evidence of nonrigid perylene having nonsymmetric oscillator loci.

On a final note, as can be seen in Figure 4, a close-up of the first 4 ps of perylene's in-plane and out-of-plane simulated depolarization demonstrates little fast libration for the "out-of-plane" rotation (displacement of a vector normal to the aromatic plane) compared to the larger fast libration for the in-plane rotation. Since the anisotropy preexponential ("β") for out-of-plane motion is also 3 times smaller, almost all of the "libration term" in $r(t)$ seen via upconversion must be in-plane motion.

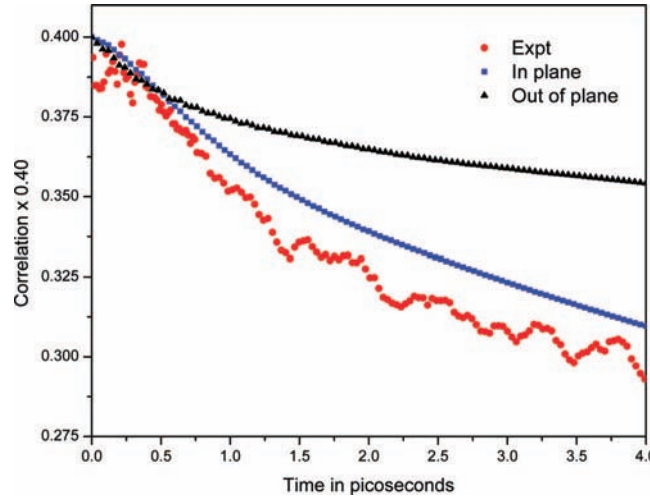

Figure 4. The first four picoseconds of the in-plane and out-of-plane simulated relaxation of perylene in hexadecane. Note the relative lack of the quasi-ballistic behavior in the out of plane rotation compared to the in-plane rotation: experiment (●, red), in-plane (■, blue), out of plane (▲, black).

4. Conclusions

The MD simulations agree well with perylene experimental results and provide insight into the existence of the fast "libration" term observed in upconversion data.

The in-plane libration of an ensemble of perylene in hexadecane can be visualized as a "wiggle" inside an average solvent pocket.[8] Perylene is able to rapidly "slip" in-plane because there is no hydrogen bonding in hexadecane, and the average solvent pocket is undisturbed by small slips. The first 30 ps of the simulation match experimental data well, and the longer decay terms in the experimental data are also mirrored. The correlation function obtained from the simulations for the out-of-plane motion of perylene contains less short-term libration than seen for the in-plane rotation, demonstrating that the libration seen in $r(t)$ is predominantly an "in-plane" phenomenon.

In contrast, for tetracene, the simulation only loosely follows the decay seen in experiments. The discrepancy could originate either in an apparent time offset (convolution artifact) or more likely in (previously reported)[2] vibrational coupling changes in this period.

Our quantum mechanical calculations of the excited states of perylene, however, affirmed that the observed behavior of perylene in hexadecane (and the recovery of the r_o defect) may be explained *using motion alone*. These quantum mechanical calculations show that neither the "twisted" nor the "butterfly" conformations of perylene should cause the r_o defect, because neither were accompanied by significant internal rotations of the transition moment that could account for loss of anisotropy. Prior studies that suggested these possibilities brought up an important alternative,[2] but a more computationally intensive examination disfavors this mechanism.

Recently, Pigliucci et al.[26] performed fluorescence upconversion experiments on perylene derivatives whose D_{2h} symmetry was broken. Their (preliminary) report invoked vibrational cooling to account for the initial decrease in anisotropy. For perylene in a noninteracting solvent (toluene), they obtained a time constant of 2.4 ps, which is 5 times slower than our measured libration rate. In tetracene and other photophysical

systems lacking the strong symmetric S_1 oscillator of perylene, vibrational cooling[2] may thus be an important consideration, but this effect was not apparent in the rise shape of "total" perylene decay curves ($I_{\|} + 2I_{\perp}$). Vibrational coupling clearly has influence on the anisotropy of some fluorophores, but it is not needed to explain our measurements of perylene motion in hexadecane. Any anisotropy decay curve calculated with libration should provide an upper envelope for experiments where both libration and cooling happen.

The fast librations seen here should be considered when analyzing, for example, orientation relaxation data obtained from tryptophans in proteins. A very fast libration was already observed in tryptophan analogs[27] that may still be operative in proteins and peptides, since tryptophan, while constrained by backbone connections, can still have molecular reorientation dominated by the "pocket" around the indole ring. We have begun femtosecond anisotropy analyses in proteins[28–30] with these effects in mind.

Acknowledgment. We received helpful advice on perylene dynamics from Mary D. Barkley, Andrzej A. Kowalczyk, and Ludwig Brand. This work was supported in part by DIR, NIH, NHLBI, and NSF Grant MCB-0133064.

References and Notes

(1) Xu, J.; Shen, X.; Knutson, J. R. *J. Phys. Chem. A* **2003**, *107*, 8383.

(2) Sarkar, N.; Takeuchi, S.; Tahara, T. *J. Phys. Chem. A* **1999**, *103*, 4808.

(3) Ehrenberg, M.; Rigler, R. *Chem. Phys. Lett.* **1972**, *14*, 539.

(4) Barkley, M.; Kowalczyk, A.; Brand, L. *J. Chem. Phys.* **1981**, *75*, 3581.

(5) Brand, L.; Knutson, J. R.; Davenport, L.; Beechem, J. M.; Dale, R. E.; Walbridge, D. G.; Kowalczyk, A. Time resolved fluorescence spectroscopy. Some applications of associative behaviour to studies of proteins and membranes. In *Spectroscopy and the Dynamics of Molecular Biological Systems*; Dale, R. E. Ed.; Academic Press: London, 1985; p 259.

(6) Zinsli, P. E. *Chem. Phys.* **1977**, *20*, 299.

(7) Mantulin, W. W.; Weber, G. *J. Chem. Phys.* **1977**, *66*, 4092.

(8) Jas, G.; Larson, E. J.; Johnson, C. K.; Kuczera, K. *J. Phys. Chem. A* **2000**, *104*, 9841.

(9) Jimenez, R.; Fleming, G. R.; Kumar, P. V.; Marncelli, M. *Nature*, **1994**, *369*, 471.

(10) Pauls, S. W.; Hedstrom, J. F.; Johnson, C. K. *Chem. Phys.* **1998**, *237*, 205.

(11) Jiang, Y.; Blanchard, G. J. *J. Phys. Chem.* **1994**, *98*, 6436.

(12) Fillaux, F. *Chem. Phys. Lett.* **1985**, *114*, 384.

(13) Christensen, R. L.; Drake, R. C.; Phillips, D. *J. Phys. Chem.* **1986**, *90*, 5960.

(14) Brocklehusrt, B.; Young, R. N. *J. Phys. Chem.* **1995**, *99*, 40.

(15) Goldie, S. N.; Blanchard, G. J. *J. Phys. Chem. A* **1999**, *103*, 999.

(16) Pauls, S. W.; Hedstrom, J. F.; Johnson, C. K. *Chemi. Phys.* **1998**, *237*, 205.

(17) Wirth, M. J.; Chou, S.-H. *J. Phys. Chem.* **1991**, *95*, 1786.

(18) Szubiakowski, J.; Balter, A.; Nowak, W.; Kowalczyk, A.; Wisniewski, K.; Wierzbowska, M. *Chem. Phys.* **1996**, *208*, 283.

(19) Shilstone, G. N.; Zannoni, C.; Verachini, C. A. *Liq. Cryst.* **1989**, *6*, 303.

(20) Brooks, B. R.; Bruccoleri, R. E.; Olafson, B. D.; States, D. J.; Swaminathan, S.; Karplus, M. *J. Comput. Chem.* **1983**, *4*, 187.

(21) Frisch, M. J.; Trucks, G. W.; Schlegel, H. B.; Scuseria, G. E.; Robb, M. A.; Cheeseman, J. R.; Montgomery, J. A., Jr.; Vreven, T.; Kudin, K. N.; Burant, J. C.; Millam, J. M.; Iyengar, S. S.; Tomasi, J.; Barone, V.; Mennucci, B.; Cossi, M.; Scalmani, G.; Rega, N.; Petersson, G. A.; Nakatsuji, H.; Hada, M.; Ehara, M.; Toyota, K.; Fukuda, R.; Hasegawa, J.; Ishida, M.; Nakajima, T.; Honda, Y.; Kitao, O.; Nakai, H.; Klene, M.; Li, X.; Knox, J. E.; Hratchian, H. P.; Cross, J. B.; Adamo, C.; Jaramillo, J.; Gomperts, R.; Stratmann, R. E.; Yazyev, O.; Austin, A. J.; Cammi, R.; Pomelli, C.; Ochterski, J. W.; Ayala, P. Y.; Morokuma, K.; Voth, G. A.; Salvador, P.; Dannenberg, J. J.; Zakrzewski, V. G.; Dapprich, S.; Daniels, A. D.; Strain, M. C.; Farkas, O.; Malick, D. K.; Rabuck, A. D.; Raghavachari, K.; Foresman, J. B.; Ortiz, J. V.; Cui, Q.; Baboul, A. G.; Clifford, S.; Cioslowski, J.; Stefanov, B. B.; Liu, G.; Liashenko, A.; Piskorz, P.; Komaromi, I.; Martin, R. L.; Fox, D. J.; Keith, T.; Al-Laham, M. A.; Peng, C. Y.; Nanayakkara, A.; Challacombe, M.; Gill, P. M. W.; Johnson, B.; Chen, W.; Wong, M. W.; Gonzalez, C.; Pople, J. A. *Gaussian; 2003*, revision B.03; Gaussian, Inc.: Pittsburgh, PA, 2003.

(22) Fourmann, B.; Jouvet, C.; Tramer, A.; Le Bars, J. M.; Millie, P. *Chem. Phys.* **1985**, *92*, 25.

(23) Schaftenaar, G.; Noordik, J. H. *J. Comput.-Aided Mol. Des.* **2000**, *14*, 123.

(24) Zimmermann, H.; Joop, N. *Elektrochem. Ber. Bunsen-Ges. Phys. Chem.* **1961**, *65*, 138.

(25) Zimmermann, H.; Joop, N. *Elektrochem. Ber. Bunsen-Ges. Phys. Chem.* **1960**, *64*, 1215.

(26) Pigliucci, A.; Vauthey, E. *Chimia* **2003**, *57*, 200.

(27) Shen, X.; Knutson, J. R. *Chem. Phys. Lett.* **2001**, *339*, 191.

(28) Xu, J.; Toptygin, D.; Graver, K.; Albertini, R.; Savtchenko, R.; Meadow, N.; Roseman, S.; Callis, P.; Brand, L.; Knutson, J. *J. Am. Chem. Soc.* **2006**, *128*, 1214.

(29) Xu, J.; Knutson, J. R. *Biophys. J.* **2003**, *84*, B647.

(30) Xu, J.; Chen, J.-J.; King, J.; Toptygin, D.; Callis, P.; Brand, L.; Knutson, J. *Biophys. J.* **2008**, *B583*, Suppl. 94, 1607.

JP7117289